Arabian Journal of Chemistry (2020) 13, 8592–8599

King Saud University

Arabian Journal of Chemistry

www.ksu.edu.sa
www.sciencedirect.com

REVIEW ARTICLE

Molecular size and shape properties of diamondoid molecules occurring in crude oil

Federico Jiménez-Cruz [*,1], **José Luis García-Gutiérrez** [*,1]

Instituto Mexicano del Petróleo, Dirección de Investigación en Transformación de Hidrocarburos, Gerencia de Separación de Hidrocarburos, Eje Central Lázaro Cárdenas Norte 152, Col. San Bartolo Atepehuacan, Gustavo A. Madero, 07730 Ciudad de México, Mexico

Received 22 July 2020; accepted 22 September 2020
Available online 24 October 2020

KEYWORDS

Diamondoids;
Adamantanes;
Diamantanes;
Molecular size;
Ovality;
B3LYP-D3/6-311 + G** calculations

Abstract The molecular size and shape for 27 diamondoids molecules (adamantanes and alkyladamantanes, diamantine and alkyldiamantanes) were calculated by computational quantum mechanical modeling method of dispersion correction B3LYP-D3/6-311 + G**, in which the family of adamantanes presents molecular sizes in terms of width of 6.8–7.9 Å, and for the family of diamantanes 6.8–7.4 Å, in terms of length the size for adamantanes are 7.6–9.5 Å and for diamantanes 9.3–10.0 Å and in terms of height are rounded from 7.4 to 9.6 Å for adamantanes and 7.4 to 8.5 Å for diamantanes. This size depends on the alkyl substitution either in CH_2 or CH bridgehead positions. A measure of spherical shape deviation in terms of ovality, (O = 1 for sphere shape) was calculated, in which for adamantane, methyladamantanes, dimethyladamantanes, and multi-substituted adamantanes, is 1.17, 1.21, 1.24, and 1.26–1.31, respectively and ovality value for diamantane is 1.20 and 1.22–1.27 for methyl substituted diamantanes. Ovality (shape) and molecular size differences between adamantane, methyladamantanes, dimethyladamantanes, multi-substituted adamantanes, and the corresponding diamantanes allow suggesting a dynamic model for separation from the linear alkanes in a mixture into a slit pore shape typical for microporous carbons.

* Corresponding authors.
E-mail addresses: jimenezf@imp.mx (F. Jiménez-Cruz), garciajl@imp.mx (J.L. García-Gutiérrez).
[1] DITH, Instituto Mexicano del Petróleo.
Peer review under responsibility of King Saud University.

ELSEVIER Production and hosting by Elsevier

https://doi.org/10.1016/j.arabjc.2020.09.043
1878-5352 Published by Elsevier B.V. on behalf of King Saud University.

Contents

1. Introduction

The isolation and identification of biomarkers are very useful in petroleum exploration technologies. The most important investigated biomarkers are hydrocarbons with intact carbon skeletons such as steroids, terpenes, or isoprenoids. Many biological markers are used in oil exploration for correlation, biodegradation, and maturity evaluations. In the same way, it is proved that molecules such as diamondoids play an important role in the evaluation of oil maturity and can be used to determine the geological origin since they are a monitor of biodegradation and thermal maturity. It is important to note that, despite their biogenic origin, diamondoids are not biomarkers in the narrow sense because they do not share structural similarities with their precursor biomolecules (Dahl et al., 2003).

The concentration of diamondoids in crude oil is about 1 to 100 ppm and is considered to be closely related to the geological maturity of an oil field (Dahl et al., 1999). Diamondoids are more stable than other hydrocarbons and are thought to be formed from polycyclic hydrocarbons under thermal stress catalyzed by a Lewis acid; thus, these molecules are resistant to thermal cracking (Wingert, 1992). Some researchers have used the relative abundances of diamondoids to estimate the degree of thermal maturity of source rocks and crude oil, especially in mature and post-mature samples (Chen et al., 1996).

For this reason, it is important to propose strategies for the isolation and separation of diamondoids and other hydrocarbons present in crude oil, gas condensates, and similar currents. These strategies involve for example: Chromatography techniques of saturated fractions and sorption–desorption by molecular recognition with β-cyclodextrin (Huang et al., 2011); selective adsorption with zeolites in the gas phase (Alexander et al., 1990); techniques for fraction enrichment by hydrotreating and catalytic hydrocracking of cuts with boiling points between 150 and 290 °C (Carlson et al., 2007); and lately by chromatography techniques using selective sorption–desorption on commercial zeolite Beta and heat treatment (Nguyen and Philp, 2016).

Also, diamondoids deserve great attention in promising applications, for example, a recent study described that methylated adamantanes were found as good candidates for optical applications due to their fluorescence brightness (Rander et al., 2017) and even some alkyl adamantanes are considered as potential enhancers for diesel because of their higher density and higher cetane features (Harvey et al., 2016).

Selective adsorption of adamantane and its methyl derivatives on graphitized carbon has been described through inverse gas chromatography (IGC) experiments, particularly on graphitized microporous carbon such as Carbopack with a grain diameter of 60/80 mesh (Yashkin et al., 2008a; Yashkin et al., 2008b). Besides, the separation of larger adamantanes such as phenyladamantane and diadamantane on the same thermally graphitized carbon has been reported (Yashkin et al., 2011).

Attracted for the high capability of graphitized microporous carbon in molecular separations, it is of particular interest to design carbon materials (Jimenez-Cruz et al., 2007; Laredo et al., 2008) for selective isolation and separation strategies for diamondoids from linear and branched paraffins occurring in crude oils, saturated fraction from SARA chromatography techniques and gas condensates. To understand the effect of molecular sieves on the separation process by molecular size and electronic interactions, we describe in this job a study of the molecular size and shape of representative adamantanes and diamantanes that naturally occurring in crude oil by computational quantum mechanical modeling method of dispersion correction B3LYP-D3/6-311 + G**.

2. Methodology

All calculations were carried out using Spartan'18 (Wavefunction Inc., Irvine, CA, USA). For modeling the diamondoids, the initial coordinates were submitted to conformational analyses at Molecular Mechanics and semiempirical AM1 level (Dewar et al., 1985). The full optimized geometry of each molecule was performed using the method of dispersion correction as an add-on to standard Kohn–Sham density functional theory B3LYP-D3 (Grimme et al., 2010) with the basis set 6-311 + G** in which B3LYP-D3 is a good correction for hydrocarbons. (Grimme, 2010). The calculations were performed using Q-Chem incorporated on Spartan'18. (Shao, et al., 2015).

Diamondoid molecular size was calculated according to a methodology described elsewhere (Jiménez-Cruz and Laredo, 2004) in which bond length and angles are readily determined from the edited optimized molecule. Corey-Pauling-Koltun (CPK) molecular volumes of the space-filling model were calculated by considering the sphere radii, being chosen as approximating van der Waals contact distances (Corey and Pauling, 1953). The measuring of the critical dimensions for diamondoids is described in Fig. 1, in which a, b and c dimensions were read from the extreme H to H distances and considering the van der Waals radii corrections for H in C-H alkane bonding, by adding to the calculated dimensions the corresponding value: 1.2 Å (Bondi, 1964).

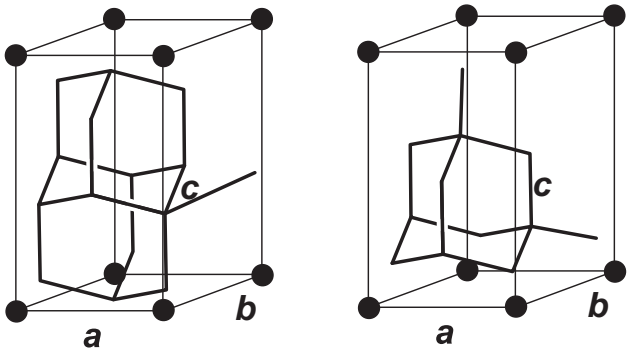

Fig. 1 Diamondoid evaluation of molecular size values.

3. Results and discussion

Critical size discrimination in the pore channels in porous materials can be predicted by taking into account pore volume, molecular CPK volume, pore diameter, critical size parameters (width, height and length), and a parameter related to the molecular shape. Diamondoids are featured by their cage tricycle molecular structure with the absence of conformational changes.

According to the procedure outlined in Section 2, the equilibrium geometry of diamondoids **1**–**27** (adamantane y diamantanes, see Figs. 2 and 3) were performed to establish the appropriate basis to determine de molecular size and other electronic parameters. In Table 1, we outline the obtained results of the calculations. The selected method, B3LYP-D3/6-311 + G** assures good results according to the recommendation found elsewhere (Grimme, 2010).

According to these results and considering the three dimensions (x, y, z) of these molecules, the family of adamantanes **1**–**17** presents molecular sizes in terms of width between 6.8 and 7.9 Å, and the family of diamantanes **18**–**27** presents molecular sizes between 6.8 and 7.4 Å, however, in terms of length the size for adamantanes is between 7.6 and 9.5 Å and for diamantanes between 9.3 and 10.0 Å. Height is rounded from 7.4 to 9.6 Å for adamantanes and 7.4 to 8.5 Å for diamantanes. This size depends on the alkyl substitution either in CH_2 or CH bridgehead positions.

A comparative plot for these molecular parameters is described in Fig. 4. Considering the molecular areas and volumes, the family of adamantanes **1**–**17** has molecular areas and volumes between 166.2 and 238.0 $Å^2$ and 159.4–230.9 $Å^3$, respectively. The diamantanes **18**–**27** family presents molecular areas and volumes between 202.8 and 251.0 $Å^2$ and 206.7–259.7 $Å^3$, respectively, showing another key critical size.

Ovality (O) is a measure of the deviation of a molecule from the spherical shape. If O = 1 the molecule shape is spherical, and O > 1 indicates the deviation of the said shape (Hehre, 2019). Ovality is described by the ratio of volume and area where A is Area and V is Volume.

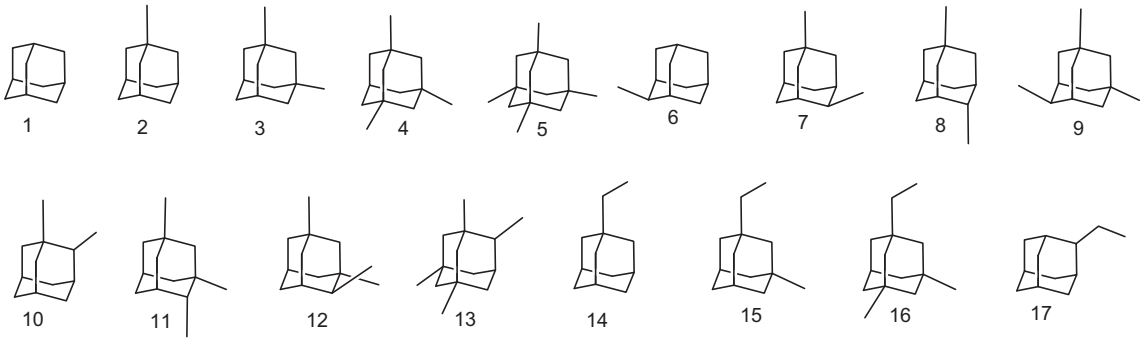

Fig. 2 Adamantane and alkyl analogs studied by B3LYP-D3/6-311 + G** theoretical method.

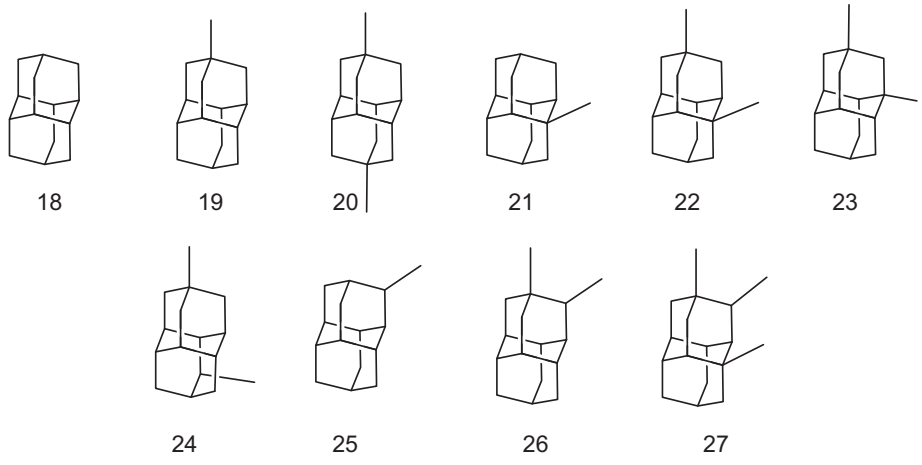

Fig. 3 Diamantane and alkyl analogs studied by B3LYP-D3/6-311 + G** theoretical method.

Table 1 B3LYP-D3/6-311 + G** results for diamondoids **1**–**27**.

	Entry	CPK molecular area (Å^2)	CPK molecular volume (Å^3)	Width (Å)	Length (Å)	Height (Å)	Ovality	Total Energy (Hartree)
1	Adamantane	166.26	159.43	6.8	7.6	7.4	1.17	-390.850805
2	1-Methyladamantane	184.23	177.19	6.8	8.5	7.4	1.21	-430.182641
3	1,3-Dimethyladamantane	202.14	195.89	6.8	8.1	7.4	1.25	-469.515206
4	1,3,5-Trimethyladamantane	220.08	212.63	7.9	9.3	7.4	1.28	-508.846464
5	1,3,5,7-Tetramethyladamantane	238.03	230.37	9.3	9.1	7.4	1.31	-548.178273
6	2-Methyladamantane	183.53	177.48	6.8	8.5	8.5	1.20	-430.177923
7	Cis-1,4-dimethyladamantane	201.58	195.19	6.8	8.5	8.3	1.24	-469.509994
8	Trans-1,4-dimethyladamantane	201.63	195.24	6.8	9.3	8.5	1.24	-469.509911
9	1,3,6-Trimethyladamantane	219.61	212.96	6.8	9.1	8.3	1.27	-508.841798
10	1,2-Dimethyladamantane	199.94	194.99	6.8	8.5	8.5	1.23	-469.507891
11	Cis-1,3,4-Trimethyladamantane	217.90	212.74	7.9	8.1	7.4	1.26	-508.840221
12	Trans-1,3,4-Trimethyladamantane	217.86	212.73	6.8	8.1	7.4	1.26	-508.840113
13	1,2,5,7-Tetramethyladamantane	235.86	230.49	8.9	9.3	8.7	1.30	-548.172122
14	1-Ethyladamantane	202.19	195.44	6.8	8.7	8.7	1.24	-469.507641
15	1-Ethyl-3-methyladamantane	219.99	213.16	6.8	9.1	8.7	1.27	-508.839469
16	1-Ethyl-3,5-dimethyladamantane	238.04	230.89	7.9	9.3	7.4	1.31	-548.171560
17	2-Ethyladamantane	202.59	195.88	6.8	9.5	9.6	1.24	-469.504366
18	Diamantane	202.79	206.79	6.8	9.3	7.4	1.20	-545.747739
19	4-Methyldiamantane	220.81	224.86	6.8	10.0	7.4	1.24	-585.079684
20	4,9-Dimethyldiamantane	238.78	242.29	6.8	10.8	7.4	1.27	-624.411654
21	1-Methyldiamantane	217.84	224.22	6.8	9.3	8.5	1.22	-585.075761
22	1,4-Dimethyldiamantane	235.84	241.95	7.4	9.3	8.5	1.26	-624.407820
23	2,4-Dimethyldiamantane	235.90	242.02	6.8	10.0	8.5	1.26	-624.407773
24	4,8-Dimethyldiamantane	238.03	242.56	6.8	10.0	8.5	1.27	-624.406932
25	3-methyldiamantane	220.11	224.84	6.8	9.3	8.5	1.23	-585.074927
26	3,4-dImethyldiamantane	236.58	242.41	6.8	10.0	8.5	1.26	-624.405170
27	1,3,4-Trimethyldiamantane	251.00	259.73	6.8	10.0	8.5	1.27	-663.732621

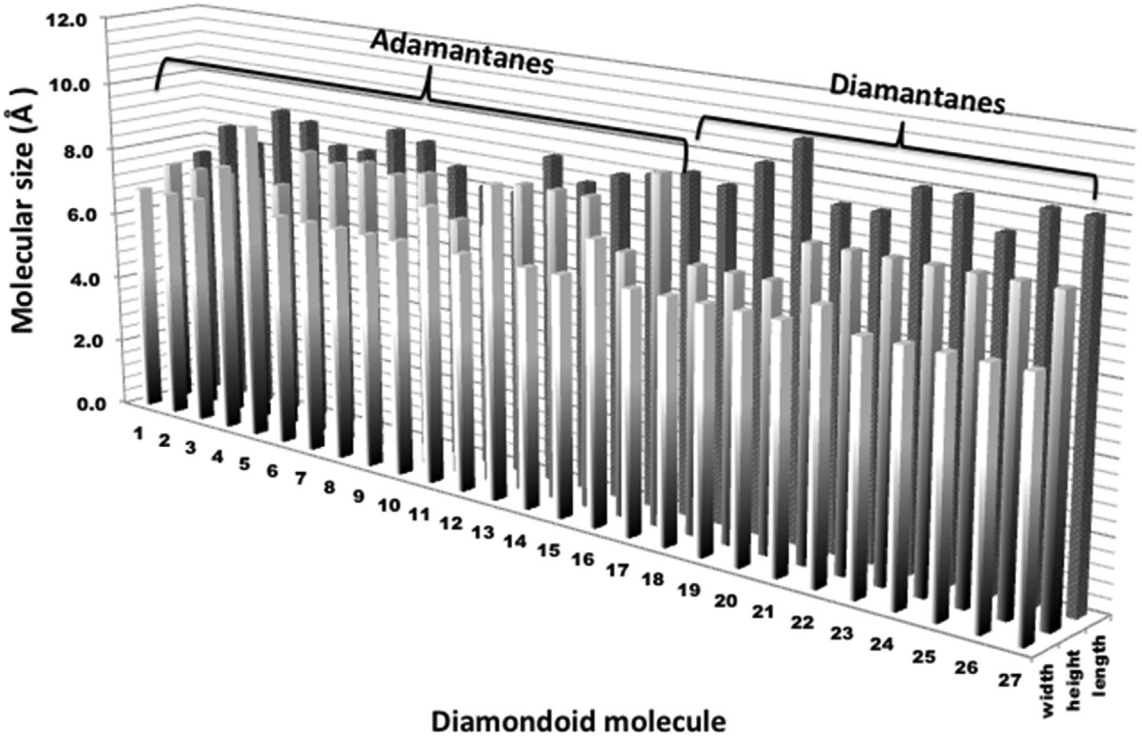

Fig. 4 Comparison plots for calculated molecular size (width, height and length) of the diamondoids **1**–**27**.

$$O = \frac{A}{4\pi\left(\frac{3V}{4\pi}\right)^{\frac{2}{3}}}$$

The calculated ovality for adamantane, methyladamantanes, dimethyladamantanes, and multi-substituted adamantanes, is 1.17, 1.21, 1.24, and 1.26–1.31, respectively (Fig. 5). The diamantanes show ovality values of 1.20 for diamantane and 1.22–1.27 for methyl-substituted diamantanes.

The concept of *minimum effective dimensions of the molecules* is a critical parameter for discriminating which dictates pore access, considers two perpendicular dimensions, either x and y dimensions of molecular size, depending on the pore shape (Webster et al., 1999). Figs. 6, 7 and 8 show correlations between ovality (shape) and the molecular size dimensions for adamantanes **1**–**17** (black circles) and diamantanes **18**–**27** (gray diamonds).

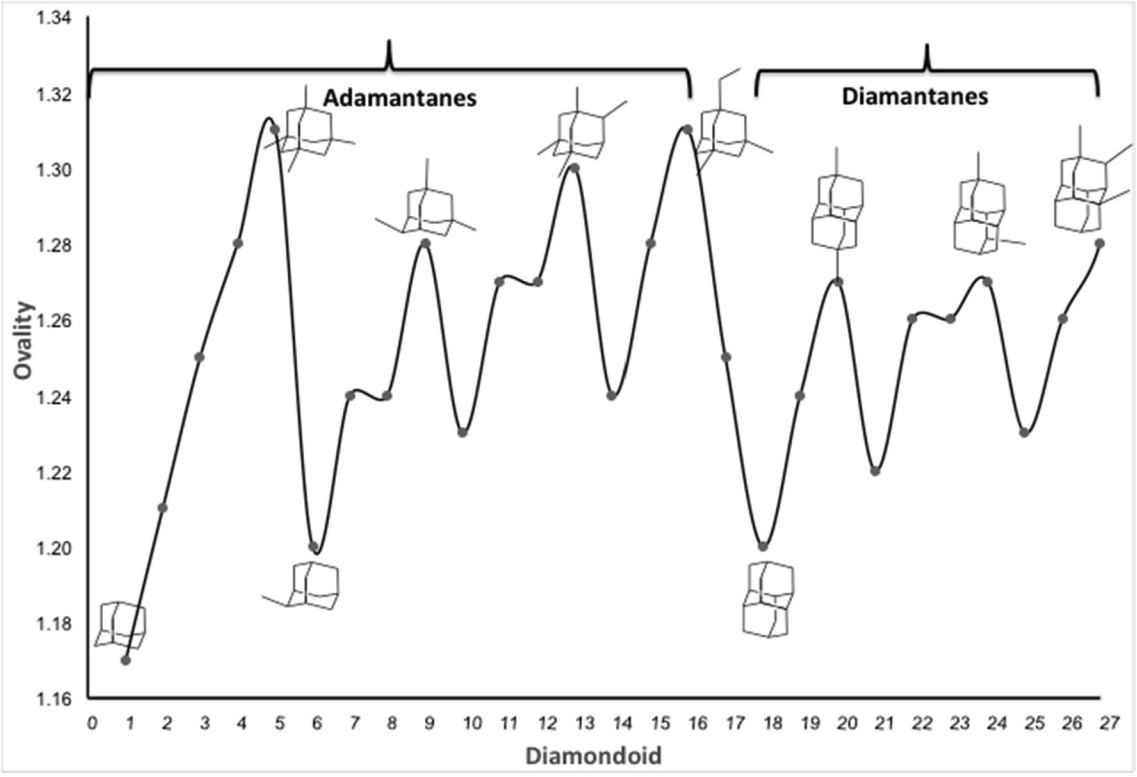

Fig. 5 Comparison plots for calculated ovality of the diamondoids **1**–**27**.

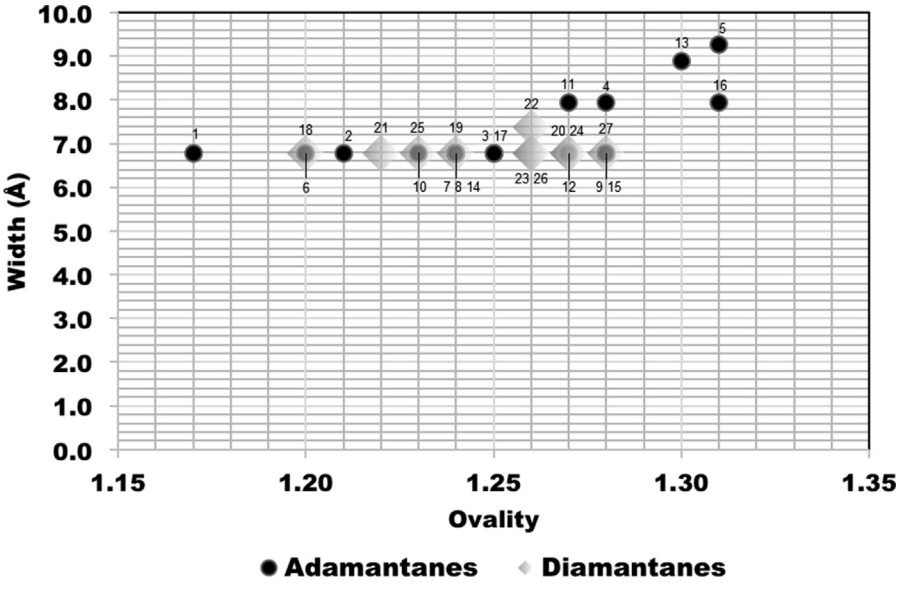

Fig. 6 Comparison plots for calculated ovality and width size dimensions of the adamantanes **1**–**17** (black circles) and diamantanes **18**–**27** (gray diamonds).

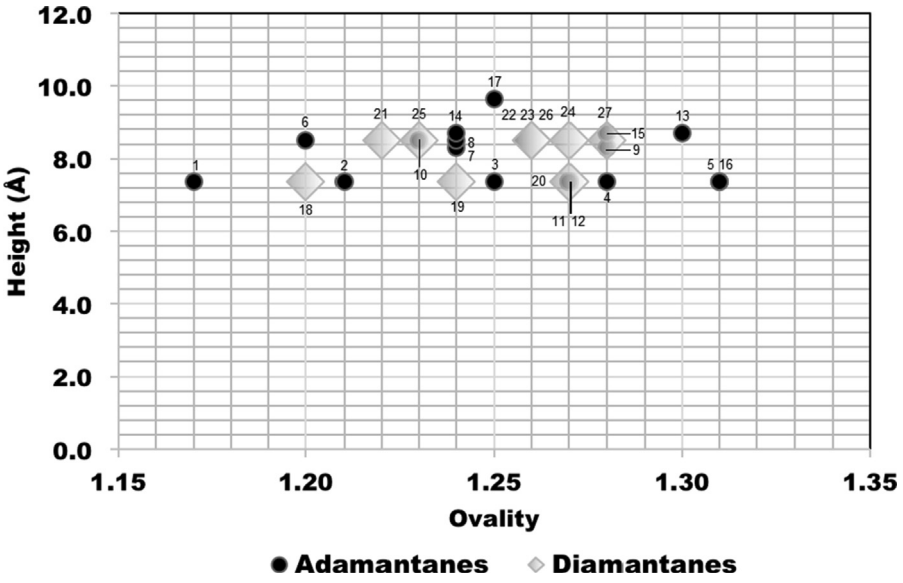

Fig. 7 Comparison plots for calculated ovality and height size dimensions of the adamantanes **1**–**17** (black circles) and diamantanes **18**–**27** (gray diamonds).

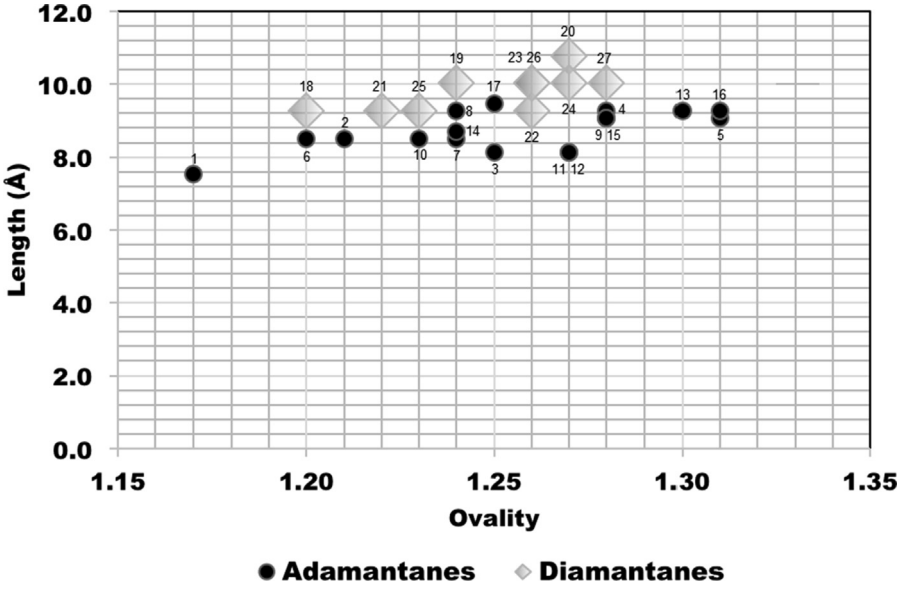

Fig. 8 Comparison plots for calculated ovality and length size dimensions of the adamantanes **1**–**17** (black circles) and diamantanes **18**–**27** (gray diamonds).

This *minimum effective dimensions of the diamondoids* can be defined by height and length. Ovality (shape) and molecular size differences between adamantane **1**, methyladamantanes, dimethyladamantanes, multi-substituted adamantanes, and the corresponding diamantanes allow suggesting a dynamic model for separation from the linear alkanes in a mixture into a slit pore shape typical for microporous carbons (Jimenez-Cruz et al., 2007).

In Fig. 9, is outlined the model for the separation of diamondoids from complex oil blends depending on the micropores size distribution and adsorption conditions. Taking into account the calculated molecular size for linear and monosubstituted paraffins of 4.2 and 5.5 Å, respectively (Jiménez-Cruz and Laredo, 2004), thus the separation of diamondoids and linear paraffins can be a plausible process in the titled adsorbent. By considering the average pore diameter value for a microporous activated carbon, 0.9148 nm (Jimenez-Cruz et al., 2007) is noticeable that size dimension and shape between alkanes and isoalkane and diamondoids are in part determinant to enter into the slit pores. The shape and size of the porous material are relevant for considering both the width and height of the molecule, diffusivity within the porous channels are controlled by any of the three limiting molecular dimensions, this behavior is known as *geometry-limited diffusion* (Shichi et al., 2001). By considering the separation of diamondoids molecules from linear alkanes, the access into

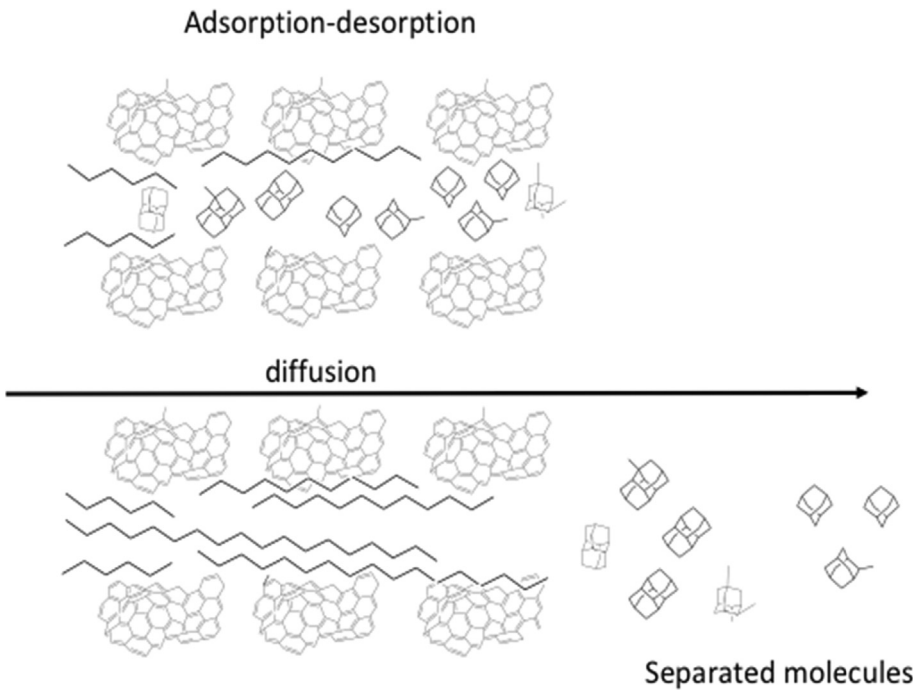

Fig. 9 Model for the separation of diamondoids from paraffins and other hydrocarbons by the gas-phase adsorption–desorption process.

two-dimensional pore structures of shorter alkanes contrasts to the longer alkanes, which only access into one-dimensional pore structure (van Well et al., 1998).

Linear paraffins have the highest affinity for microporous carbon in contrast to diamondoids due to differences in size and shape in diffusion in gas phase separations (Jimenez-Cruz et al., 2007; Laredo et al., 2008).

4. Conclusions

The molecular size and shape for 27 diamondoids molecules (adamantanes, alkyladamantanes, diamantine, and alkyldiamantanes) were calculated by B3LYP-D3/6-311+G** quantum chemical calculations, in which the family of adamantanes presents molecular sizes in terms of width between 6.8 and 7.9 Å, and the family of diamantanes presents molecular sizes between 6.8 and 7.4 Å, in terms of length the size for adamantanes are between 7.6 and 9.5 Å and for diamantanes between 9.3 and 10.0 Å. For height are rounded from 7.4 −9.6 Å for adamantanes and 7.4–8.5 Å for diamantanes. This size depends on the alkyl substitution either in CH_2 or CH bridgehead positions. A measure of spherical shape deviation (Ovality, O) was calculated, in which for adamantane, methyladamantanes, dimethyladamantanes, and multi-substituted adamantanes, is 1.17, 1.21, 1.24, and 1.26–1.31, respectively and ovality value for diamantane is 1.20 and 1.22–1.27 for methyl substituted diamantanes. The *minimum effective dimensions of the diamondoids* can be defined by height and length. Ovality (shape) and molecular size differences between adamantane, methyladamantanes, dimethyladamantanes, multi-substituted adamantanes, and the corresponding diamantanes allow suggesting a dynamic model for separation from the linear alkanes in a mixture into a slit pore shape typical for microporous carbons.

Declaration of Competing Interest

The authors declare that they have no known competing financial interests or personal relationships that could have appeared to influence the work reported in this paper.

Acknowledgement

This work was supported by IMP funds.

References

Alexander, R.A., Knight, C.E., Whitehurst, D.D., 1990. Removal of diamondoid compounds from hydrocarbonaceous fractions. US Patent 4952749 A.

Bondi, A., 1964. van der Waals Volumes and Radii. J. Phys. Chem. 68, 441–451. https://doi.org/10.1021/j100785a001.

Carlson, R.M., Dahl, J.E., Liu, Sh., Maesen, T., Qureshi, W.R., Kyung, H., Timken, C., 2007. Processes for concentrating higher diamondoids. US Patent 7173160 B2.

Chen, J., Fu, J., Sheng, G., Liu, D., Zhang, J., 1996. Diamondoid hydrocarbon ratios: novel maturity indices for highly mature crude oils. Org. Geochem. 25, 179–190. https://doi.org/10.1016/S0146-6380(96)00125-8.

Corey, R.B., Pauling, L., 1953. Molecular Models of Amino Acids, Peptides, and Proteins. Rev. Sci. Instr. 24, 621–627. https://doi.org/10.1063/1.1770803.

Dahl, J.E.P., Moldowan, M., Torren, M., Peakman, J.C., Clardy, E., Lobkovsky, M.M., Olmstead, M.P.W., Davis, T.J., Steeds, J.W., Peters, K.E., Pepper, A., Ekuan, A., Carlson, R.M.K., 2003. Isolation and Structural Proof of the Large Diamond Molecule, Cyclohexamantane ($C_{26}H_{30}$). Angew. Chem. Int. Ed. 42, 2040–2044. https://doi.org/10.1002/anie.200250794.

Dahl, J.E.P., Moldowan, J.M., Peters, K.E., Claypool, G.E., Rooney, M.A., Michael, G.E., Mello, M.R., Kohnen, M.L., 1999. Diamondoid hydrocarbons as indicators of natural oil cracking. Nature. 399, 54–57. https://doi.org/10.1038/19953.

Dewar, M.J.S., Zoebisch, E.G., Healy, E.F., Stewart, J.J.P., 1985. Development and use of quantum mechanical molecular models. 76. AM1: a new general purpose quantum mechanical molecular model. J. Am. Chem. Soc. 107, 3902–3909. https://doi.org/10.1021/ja00299a024.

Grimme, S., 2010. n-Alkane Isodesmic Reaction Energy Errors in Density Functional Theory Are Due to Electron Correlation Effects. Org. Lett. 12 (20), 4670–4673. https://doi.org/10.1021/ol1016417.

Grimme, S., Antony, J., Ehrlich, S., Krieg, H., 2010. A consistent and accurate ab initio parametrization of density functional dispersion correction (DFT-D) for the 94 elements H-Pu. J. Chem. Phys. 132, 154104–154119. https://doi.org/10.1063/1.3382344.

Harvey, B.G., Harrison, K.W., Davis, M.C., Chafin, A.P., Baca, J., Merriman, W.W., 2016. Molecular Design and Characterization of High-Cetane Alkyl Diamondoid Fuels. Energy Fuels 30, 10171–10178. https://doi.org/10.1021/acs.energyfuels.6b01865.

Hehre, W.J., 2019. Spartan '18 Tutorial and Users Guide Irvine CA: Wavefunction, Inc. ISBN 978-1-890661-43-0.

Huang, L., Zhang, Sh., Wang, H., Fu, X., Zhang, W., Xu, Y., Wei, C., 2011. A novel method for isolation of diamondoids from crude oils for compound-specific isotope analysis. Org. Geochem. 42, 566–571. https://doi.org/10.1016/j.orggeochem.2011.02.010.

Jiménez-Cruz, F., Laredo, G.C., 2004. Molecular size evaluation of linear and branched paraffins from the gasoline pool by DFT quantum chemical calculations. Fuel 83, 2183–2188. https://doi.org/10.1016/j.fuel.2004.06.010.

Jimenez-Cruz, F., Hernández, J.A., Laredo, G.C., Mares-Gallardo, M. T., García-Gutiérrez, J.L., 2007. Adsorption of n-Heptane and 2-Methylheptane in the Gas Phase on Polyvinylidene Chloride-Based Microporous Activated Carbon. Energy Fuels 21, 2929–2934. https://doi.org/10.1021/ef070072c.

Laredo, G.C., Meneses, E., Castillo, J., Marroquin, J.O., Jimenez-Cruz, F., 2008. Adsorption Equilibrium and Kinetics of Branched Octane Isomers on a Polyvinylidene Chloride-Based Carbon Molecular Sieve. Energy Fuels 22, 2641–2648. https://doi.org/10.1021/ef7006408.

Nguyen, T.X., Philp, R.P., 2016. Separation of diamondoids in crude oils using molecular sieving techniques to allow compound-specific isotope analysis. Org. Geochem. 95, 1–12. https://doi.org/10.1016/j.orggeochem.2016.02.005.

Rander, T., Bischoff, T., Knecht, A., Wolter, D., Richter, R., Merli, A., Möller, T., 2017. Electronic and Optical Properties of Methylated Adamantanes. J. Am. Chem. Soc. 139, 11132–11137. https://doi.org/10.1021/jacs.7b05150.

Shao, Y., Gan, Zh., Epifanovsky, E., Gilbert, A., Wormit, M., Kussmann, J., Lange, A., Behn, A., Deng, J., Feng, X., Ghosh, D., Goldey, M., Horn, P., Jacobson, L., Kaliman, I., Khaliullin, R., Kuś, T., Landau, A., Liu, J., Head-Gordon, M., 2015. Advances in Molecular Quantum Chemistry Contained in the Q-Chem 4 Program Package. Mol. Phys. 113, 184–215. https://doi.org/10.1080/00268976.2014.952696.

Shichi, A., Satsuma, A., Hattori, T., 2001. Influence of hydrocarbon molecular size on the selective catalytic reduction of NO by hydrocarbons over Cu-MFI zeolite. Appl. Catal. A. 207, 315–321. https://doi.org/10.1016/S0926-860X(00)00661-X.

van Well, W.J.M., Cottin, X., de Haan, J.W., Smit, B., Nivarthy, G., Lercher, J.A., van Hoff, J.H.C., van Santen, R., 1998. Chain Length Effects of Linear Alkanes in Zeolite Ferrierite. 1. Sorption and ^{13}C NMR Experiments. Phys. Chem. B 102, 3945–3951. https://doi.org/10.1021/jp980398+.

Webster, C.E., Drago, R.S., Zerner, M.C., 1999. A method for characterizing effective pore sizes of catalysts. J. Phys. Chem. B 103, 1242–1249. https://doi.org/10.1021/jp984055n.

Wingert, W.S., 1992. G.C.-M.S. analysis of diamondoid hydrocarbons in Smackover petroleums. Fuel. 71, 37–43. https://doi.org/10.1016/0016-2361(92)90190-Y.

Yashkin, S.N., Novoselova, O.V., Svetlov, D.A., 2008a. The thermodynamic characteristics of adsorption and retention of adamantane derivatives on graphitized carbon black under the conditions of gas-adsorption chromatography. Russ. J. Phys. Chem. A 82, 849–854. https://doi.org/10.1134/S0036024408050270.

Yashkin, S.N., Svetlov, D.A., Novoselova, O.V., Yashkina, E.A., 2008b. Experimental and molecular statistical study of alkyladamantane adsorption on graphitized thermal carbon black. Russ. Chem. Bull. Int. Ed. 57, 2472–2482. https://doi.org/10.1007/s11172-008-0356-5.

Yashkin, S.N., Svetlov, D.A., Sarkisova, V.S., 2011. Adsorption of isomeric aryl- and diadamantane molecules on the surface of graphitized thermal carbon black. Russ. Chem. Bull. Int. Ed. 60, 1814–1819. https://doi.org/10.1007/s11172-011-0274-9.